Designing superhydrophobic surfaces using fluorosilsesquioxane-urethane hybrid and porous silicon gradients

Aravindaraj G. Kannan[a], Steven J. P. McInnes[b], Namita R. Choudhury*[a], Naba K. Dutta[a], Nicolas H. Voelcker[b]

[a] Ian Wark Research Institute, University of South Australia, Mawson Lakes, SA, Australia;
[b] School of chemistry, Physics and Earth Sciences, Flinders University, Adelaide, SA, Australia

*e-mail: Namita.choudhury@unisa.edu.au, phone: 61 8 8302 3719, fax: 61 8 8302 3683

ABSTRACT

Here we describe a new class of near superhydrophobic surfaces formed using fluorinated polyhedral oligosilsesquioxane (FluoroPOSS) urethane hybrids and porous silicon gradients (pSi). We demonstrate that the surface segregation behavior of the hydrophobic fluoro component can be controlled by the type and nature of chain extender of the urethane and resultant hydrophobic association via intra or intermolecular aggregation. The surface film formed exhibits near superhydrophobicity. This work has significant potential for applications in antifouling and self-cleaning coatings, biomedical devices, microfluidic systems and tribological surfaces.

Keywords: FluoroPOSS, superhydrophobicity, silsesquioxanes, porous gradients, urethane hybrid

1. INTRODUCTION

The wettability of a solid surface is an important consideration in surface science. Modulation of wettability is important in such applications as self-cleaning coatings, biomedical devices, tribological surfaces and microfluidic systems [1-3]. Control over wettability is achieved by altering the surface chemical composition and topology. In recent years, considerable attention has been directed towards preparing superhydrophobic surfaces (water contact angle, WCA >150°) by mimicking the lotus leaf, which exhibits water contact angle of 150° or more and low contact angle hysteresis. The "lotus leaf effect" stems from the unique microscopic roughness produced by the hydrophobic epicuticular wax crystalloids positioned on the surface of each leaf [4]. Artificial surfaces exhibiting similar behaviour can be fabricated via two methods [5]; namely (1), creating micro/nanoscale roughness on a hydrophobic substrate surface or (2) by incorporating a thin layer of hydrophobic thin film on a micro/nanoscale patterned or textured surfaces. This paper focuses on the second method of surface preparation.

Many studies have focused on creating hydrophobic fluorocarbon containing surfaces using self-assembled monolayers (SAMs) [6], blends [7], copolymers [8] and functional nanoparticles [9]. Polyhedral compounds are also candidates for creating such surfaces because of their molecular scale roughness and hydrophobicity. Amongst various types of polyhedral compounds, polyhedral oligomeric silsesquioxane (POSS) based materials have attracted significant interest due to their versatility stemming from high thermal stability, oxidation resistance, discrete molecular weight and controllable functionalization. POSS is a class of nanostructured material characterized by an inorganic silicon-oxygen core surrounded by organic and/or

Smart Materials V, edited by Nicolas H. Voelcker, Helmut W. Thissen,

reactive functionalities. When one or more of the peripheral groups is replaced with fluorocarbon chains, the resulting fluorinated POSS exhibits interesting surface and bulk properties [10-12]. Moody *et al* [11] blended fluorinated and non-fluorinated POSS nanostructures with different matrices and showed that the fluorinated POSS segments drastically increased the hydrophobicity and oleophobicity of the resulting materials. In another study, Tuteja *et al* [13] fabricated superhydrophobic surfaces using fluorodecylPOSS-polymethylmethacrylate electrospun fibers. Recently, we have reported [14] the fabrication of hydrophobic fluorosilsesquioxane-urethane hybrid thin film on flat silicon wafer substrates. The resulting film was very smooth with a roughness value of 5-6 nm and this study revealed the absence of any surface roughness contribution towards the hydrophobicity. This indicates that the trapping of air in the surface fractal structure of the film was not sufficient to cause superhydrophobicity as per Cassie's law (equation 1):

$$\mathrm{Cos}\theta_c = \varphi_1 \mathrm{Cos}\theta_1 + \varphi_2 \mathrm{Cos}\theta_2 \quad (1)$$

where θ_c – observed contact angle, φ_1, φ_2 – surface area fraction of components 1 and 2, θ_1, θ_2 – contact angle of flat film of components 1 and 2. Thus when component 2 is air, $\theta_2 = 180°$, $\mathrm{Cos}\theta_c = \varphi_1 (\mathrm{Cos}\theta_1 + 1) - 1$, which indicates a material with small φ_1 and large θ_1, will display superhydrophobic behavior.

Hence, to achieve surfaces with superhydrophobic properties (contact angle > 150°) surface structure also needs to be considered [15]. The surface should contain roughness on various length scales to make them superhydrophobic. Since hydrophobicity and nanometer scale roughness are achieved with FluoroPOSS coatings; we expect the application of these hybrid thin films on micro-scale textured substrates to result in near superhydrophobic surfaces. Porous silicon (pSi) is one of the most promising candidates for the preparation of micro-textured surfaces. pSi exhibits interesting properties such as biocompatibility and highly tunable optical properties. This has created enormous interest in the scientific community for applications such as optical mirrors, waveguides [16] and biosensors [1, 17]. The surface chemistry of this material can be modified with hydrophobic or hydrophilic segments [18], which can be exploited to prepare superhydrophobic surfaces. In addition, the dimensions of the porous structures can be varied to prepare texture gradients, which would allow the examination of spectrum of effects within a single sample surface.

Therefore, in this work, we have utilized open caged Fluoro (13) disilanol isobutyl-POSS structure (given in Scheme 1 and, henceforth referred as FluoroPOSS), containing two functional hydroxyl groups, which can react with isocyanate containing monomers to form urethane linkages. The prepared hybrids and the FluoroPOSS monomers are used to chemically modify the pSi gradients in an attempt to form superhydrophobic surfaces. Also, the effects of pore size on the surface wettability are elucidated.

2. MATERIALS AND METHODS

2.1 Synthesis of Fluorosilsesquioxane-urethane Hybrid

Fluorosilsesquioxane-urethane hybrid was prepared using two-step polyurethane reaction by reacting 2,2,3,3,4,4,5,5-octafluoro-1,6-hexanediol (OFHD) and hexamethylene diisocyanate (HDI) at a stoichiometric molar ratio of 1:2.2 (OFHD: HDI) in the first step followed by chain extension with Fluoro (13) disilanol isobutyl-POSS (molecular weight – 1195 AMU). Anhydrous tetrahydrofuran (THF) and dibutyl tin dilaurate (DBTDL) were used as solvent and catalyst respectively and the reaction was carried out at 75±1 °C. This hybrid is henceforth referred as Hybrid-1. Also, another hybrid (Hybrid-2) was prepared by reacting FluoroPOSS with HDI in the first step reaction and OFHD as chain extender. The progress of the reaction was monitored using transmission Fourier Transform infrared spectroscopy (FTIR) from the decrease in the isocyanate peak. Detailed description of the synthesis and characterization of the hybrids has been previously described [14, 19].

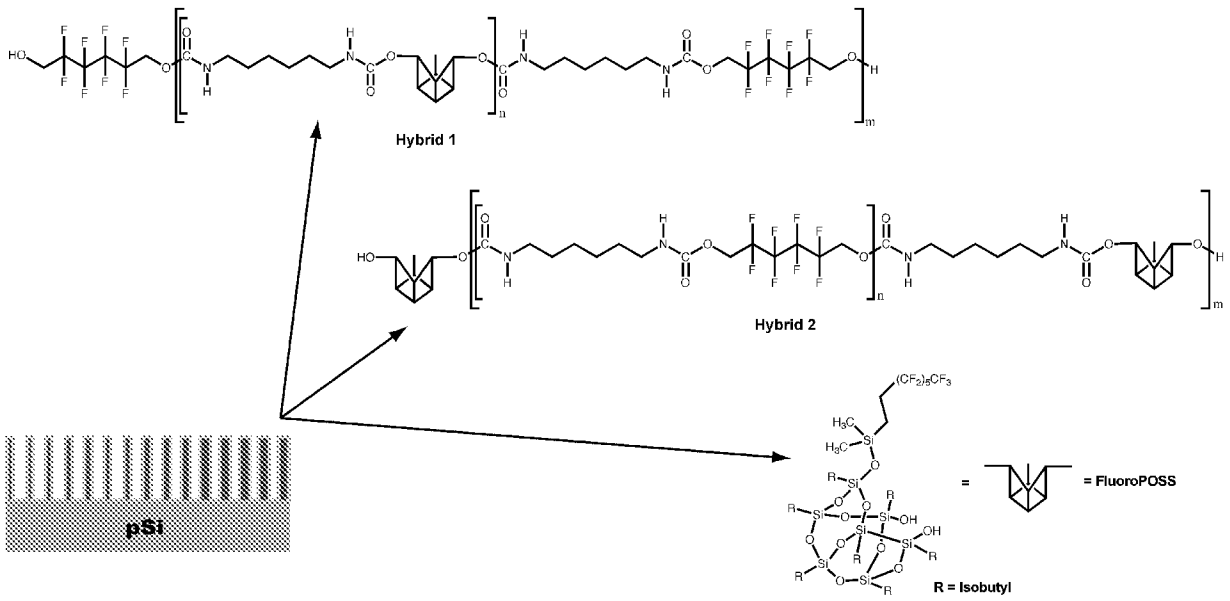

Scheme 1: Structure of FluoroPOSS and both hybrids used for the dip coating of pSi.

2.2 pSi Gradient Preparation

pSi samples were prepared from p-type (boron-doped) silicon wafers with (100) orientation and resistivity of 0.0005-0.001 Ω cm (Virginia Semiconductors). Samples were prepared in the setup similar to that as previously described [20]. Briefly, surfaces were etched by placing the electrode perpendicular to the surface on one end of a Teflon well in a 1:1 (v/v) solution of 49 % aqueous HF/ethanol for 90 seconds at a constant current density. Three currents were applied: 40 mA, 50 mA and 60 mA over a surface area of 1.767 cm^2, giving current densities of 22.64 mA cm^{-2}, 28.31 mA cm^{-2} and 33.40 mA cm^{-2} respectively. After etching, the samples were rinsed with ethanol and dichloromethane and dried under a stream of N_2. The freshly etched pSi surfaces were thermally oxidised in a tube furnace at 600 °C for 1 h. After oxidation, the surfaces were rinsed extensively with ethanol and dried under a stream of N_2.

2.3 Thin Film Coating

Thermally oxidized pSi samples were dip-coated by immersion in by 1% m/v partially reacted (at 75% isocyanate consumption) hybrid solutions in dry THF for 2 min and then dried with pure nitrogen. Similarly, FluoroPOSS films were formed on treated silicon wafers using 1% m/v FluoroPOSS solution in dry THF for 2 min by dip-coating. The coated samples were placed in an oven at 80 °C for 1 week for curing. The post cured coated samples were dried and then utilized for further surface characterizations.

2.4 Water Contact Angle Analysis

The static WCA was measured by placing a small drop (1 μL) of MilliQ water onto the sample surface via a syringe, a digital image of which was taken by a Panasonic SuperDynamic WV-BP550/G camera with a macrolens. The image was processed by ImageJ software V1.34. All reported water contact angles are the average value of at least three measurements on different parts of the sample.

2.5 FTIR-ATR

FTIR-ATR was performed on a Thermo-Nicolet Nexus 870. 64 scans were taken at room temperature and atmospheric pressure with a resolution of 4 cm^{-1}. The data was collected in the range of 625-3500 cm^{-1}, and analysed using OMNIC version 7.0 software.

2.6 Spectroscopic Characterization

X-ray photoelectron spectroscopy (XPS) was carried out using Kratos Axis Ultra Spectrometer, equipped with an Al-Kα X-ray source (hν=1486.7 eV). Hybrid thin films on pSi surfaces and the thin film on pSi prepared using FluoroPOSS monomer were characterized at a photoelectron take-off angle of 90° to the sample surface. Charge correction was performed by fixing the hydrocarbon component of C 1s peak to 284.6 eV. Data obtained were analyzed using CasaXPS processing software.

3. RESULTS AND DISCUSSION

3.1 Surface Modification

Surface modification of the thermally oxidized pSi samples are characterized using X-ray photoelectron spectroscopy (XPS). The comparison of the theoretical chemical composition (calculated based on the stoichiometric feed ratio of the monomers) with the surface chemical composition determined from XPS analysis is given in Table 1. As expected, pSi surface shows the presence of prominent peaks of silicon and oxygen. The presence of a strong peak of oxygen confirms the formation of fresh oxide layer on the electrochemically etched pSi gradients. The fresh oxide layer permits chemical bonding with the hydroxyl groups of the hybrid urethane and the FluoroPOSS monomer. The FluoroPOSS monomer modified surface shows the presence of fluorine and carbon along with silicon and oxygen. The detected fluorine and carbon peaks arise from the peripheral isobutyl group and fluorocarbon chain of the FluoroPOSS nanostructure, which confirms the presence of these structures on the surface. In case of hybrid coated samples, the spectra show the presence of all the above-mentioned elements along with nitrogen. The nitrogen peak observed in the hybrid coated samples indicates the presence of urethane linkages. The experimentally determined values of carbon, fluorine and nitrogen are much lower than the theoretically expected values. In contrast the experimental values of oxygen are significantly higher than the theoretical values. Silicon experimental values are marginally higher than expected. The presence of a strong oxygen peak in all the coated samples may indicate that the oxygen signal arises from both the oxide layer on the surface of pSi and from the thin film coating. This would suggest that the thickness of the formed film on pSi is 7 nm or less, the accepted sensitivity of this technique. To confirm this result and to understand the oxidation states of carbon, high-resolution spectra of the C 1s regions were obtained.

Table 1: XPS survey spectra data of coated and uncoated pSi gradient surfaces

Element	% Composition						
	pSi	FluoroPOSS		Hybrid-1		Hybrid-2	
		Theor. %	Exptl. %	Theor. %	Exptl. %	Theor. %	Exptl. %
C	1.61	40.75	20.43	42.67	30.88	42.67	26.13
F	-	22.07	8.01	23.65	14.71	23.65	13.93
N	-	-	-	3.31	1.02	3.31	1.56
Si	25.58	20.01	20.03	13.27	15.27	13.27	16.28
O	72.8	17.15	51.52	17.07	38.1	17.07	42.08

The C 1s spectrum of FluoroPOSS thin film shows four peaks centered at 284.6 eV, 286.4 eV, 291.7 eV and 294.1 eV (Figures 1 (a) and (b) respectively). The peak at 284.6 eV is attributed to the carbon bound to carbon and hydrogen (C-C, C-H), whereas the peak at 286.4 eV is attributed to the carbon making a single bond with oxygen (C-O). The major peak at 284.6 eV indicates the presence of aliphatic carbon atoms from the hexamethyl groups in the hybrid and also from the isobutyl groups in the periphery of the FluoroPOSS cage structure. The C-O bond arises from the fresh oxide layer formed on the pSi gradient. The other two peaks at

291.7 eV and 294.1 eV are attributed to CF_2 and CF_3 groups of the fluorocarbon chain in the periphery of the FluoroPOSS structure respectively. The Hybrid-1 C 1s spectrum shows the peaks corresponding to all the above-mentioned components along with a new peak at 288.4 eV. The peak at this binding energy (288.6 eV) is due to the carbon making one single bond and one double bond with oxygen (O=C-O) [21-23]. This arises from the carbonyl group of the urethane linkage (-NHCOO-), confirming the formation of fluorosilsesquioxane-urethane hybrid thin film on the surface of pSi gradients.

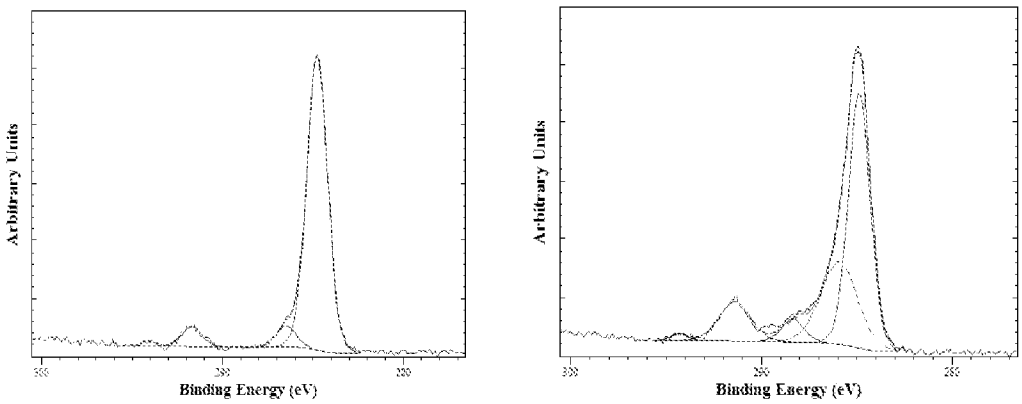

Figure 1: High resolution C 1s spectra of (a) FluoroPOSS thin film and (b) Hybrid-1 thin film

Infrared analysis was also performed on the modified surfaces (Figure 2). The FluoroPOSS coated surface (Fig 2(A)) showed very few significant peaks while Hybrids 1 and 2 (Figure 2 (B) and (C) respectively) showed a dramatic increase in multiple regions, namely at 1710 cm^{-1} and 1640 cm^{-1} for the carbonyl and amide functionalities in the urethane linkages. There is also an increase in the 3350 cm^{-1} region, which is indicative of the amide N-H stretch. The peak at 1250 cm^{-1} present in all 3 spectra has also increased for the two Hybrid coatings and this is attributed to the C-F alkyl stretching of the OFHD chain extender. The spectra also displayed C-H stretching vibrations between 2850 and 3000 cm^{-1} however these have been excluded along with the Si-O stretch at 1100 cm^{-1} to increase the clarity of the spectra shown.

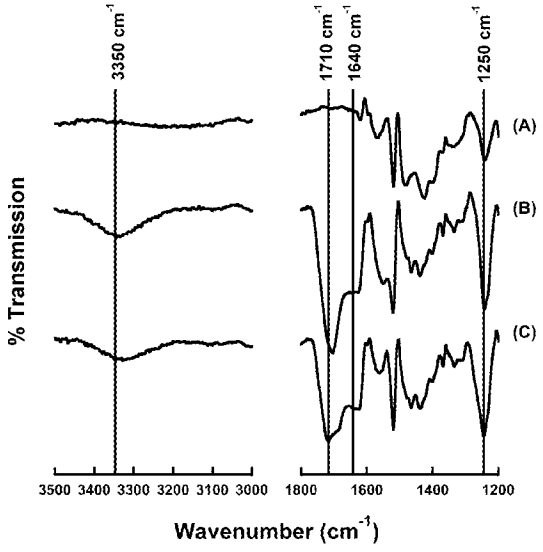

Figure 2: FTIR-ATR of (A) FluoroPOSS coated pSi, (B) Hybrid 1 coated pSi and (C) Hybrid 2 coated pSi.

3.2 Morphological Characterization

The topography of the freshly prepared pSi gradient surfaces is presented in a previous publication [18]. In order to study the effect of pore sizes on the wettability of the surfaces, the pSi gradient is divided into three regions: namely large, medium and small pores based on the pore size created on the pSi surfaces as the current moves away from the Pt electrode. As the pore characteristics have been previously described [18] we briefly characterized the newly created dip-coated surfaces via AFM (Fig. 3), in order to confirm that the pores remain open with our dip coatings.

Figures 3 (A), (B) and (C) show the AFM topographic images of Hybrid-1 thin film on large, medium and small pore regions of a 60 mA pSi gradient respectively. These images show uniform distribution of pores throughout the sample surface and differential pore size formation depending on the distance from the counter electrode.

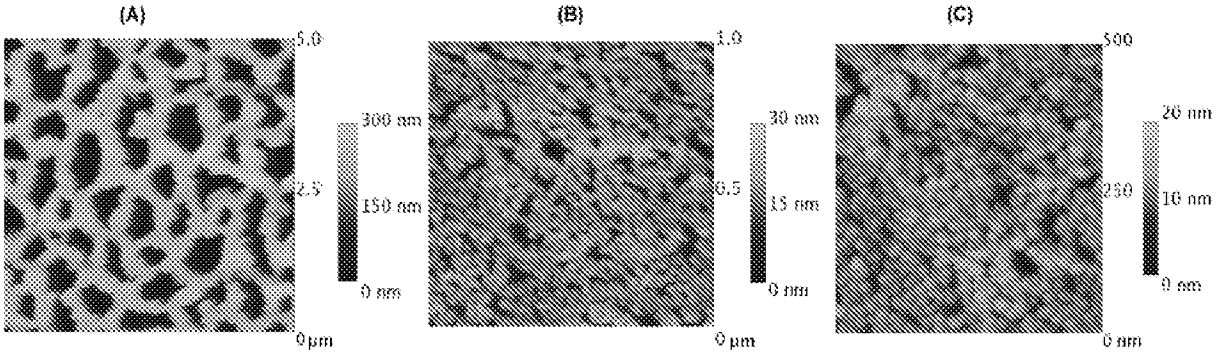

Figure 3: Topographic images of a Hybrid-1 coated 60 mA lateral pSi gradient in the (a) large, (b) medium and (c) small pore size regions.

Previously [18] we graded the corresponding pore size regimes in the following manner from largest to smallest; 60 mA Large (3000-1000 nm), 60 mA Medium (1000-300 nm), 60 mA Small (700-300 nm). It is important to note that the pore sizes characterized here (ca. 1000 nm, 150 nm and 50 nm) are smaller than those previously characterized. This could be due to the presence of the Hybrid-FluoroPOSS dip coatings, wafer-to-wafer doping variation causing pore size variations during anodisation or different position selection for analysis. However, we have assumed that these effects will be constant over all surfaces and therefore we have continued to use our previous assessment of the pore size regimes.

3.3 Contact Angle Analysis

To best understand the combination of both pore size and surface chemistry on the hydrophobicity of our surfaces we investigated the contact angle of each surface coating on a flat silicon substrate. The introduction of the various polymer layers dramatically increased the hydrophobicity even on flat substrates (Figure 4). The FluoroPOSS surface was the least hydrophobic reaching a contact angle of approximately 85°, this however, is still a substantial increase from a contact angle of 44° for untreated flat silicon. Hybrid 1 and Hybrid 2 also showed a substantial increase in contact angle, with hybrid 2 having an average contact angle of around 100° (an increase of approximately 56°). Our previous more extensive study [19] of the various fluoro-polymers on flat Si substrates by advancing contact angle has shown even higher contact angles of approximately 100-110°. The contact angle of oxidized porous silicon is around 11°, this is due to the hydrophilic nature of the surface actually drawing water into the pores and dramatically decreasing the contact angle. This effect is explained by the Wenzel model [24] and as others have found in previous work the larger the pore volume, the more water from the droplet can enter into the porous surface [25-27].

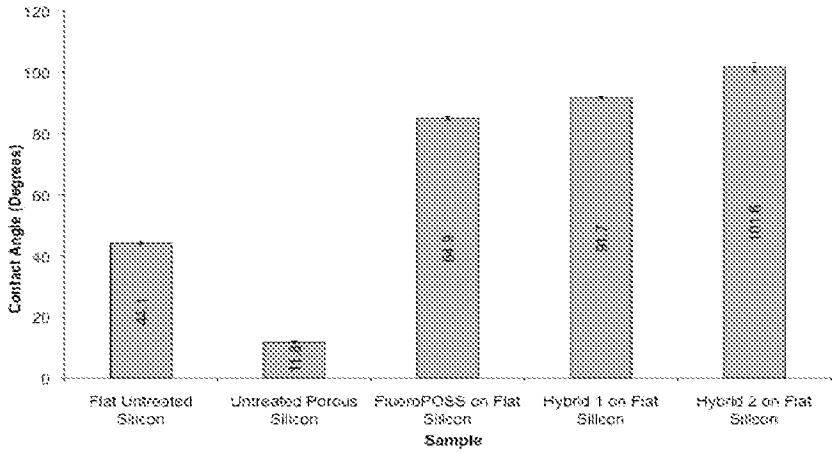

Figure 4: Static contact angle analysis results of uncoated silicon, uncoated oxidised pSi and FluoroPOSS, Hybrid 1 and Hybrid 2 coated flat silicon surfaces (error bars shown are +/- the standard deviation)

Next, static contact angle measurements were performed on all pore regions to investigate the hydrophobicity achieved by combining pore size and coating conditions. From comparing the flat samples (Figure 4) and the porous samples (Figure 5) we can see that there is a small but noticable increase for all surface coatings on the smallest pore region (40 mA small, < 5 nm pores). However a more dramatic effect is seen from the introduction of the porous layer if we compare the contact angles of each surface functionalisation on the largest pore region (60 mA Large, 1000 nm pores) with those obtained on the flat silicon; FluoroPOSS increases from 85° to 108° (a 23° change), Hybrid 1 increases from 91° to 111° (a 20° change) and Hybrid 2 increases from 102° to 130° (a 28° change). The static contact angle measurement on each surface demonstrates that the FluoroPOSS surface is the least hydrophobic (Figure 5). It is likely that this is due to the absence of the fluorine containing OFHD chain extender from this surface preparation. Both hybrid 1 and 2 contain the OFHD either as a chain extender or as a precursor and both show a significant increase in static contact angle. It is also clear that the larger pore sizes present on the 60 mA surface lead to an increase in the surface hydrophobicity. This effect is described by the Cassie-Baxter Model [28]. These increases in contact angle (ca. 105 – 130°) for Hybrid 2 are comparable to the increase seen on our fluorosilane functionalized surfaces (ca. 114 – 125°) [18].

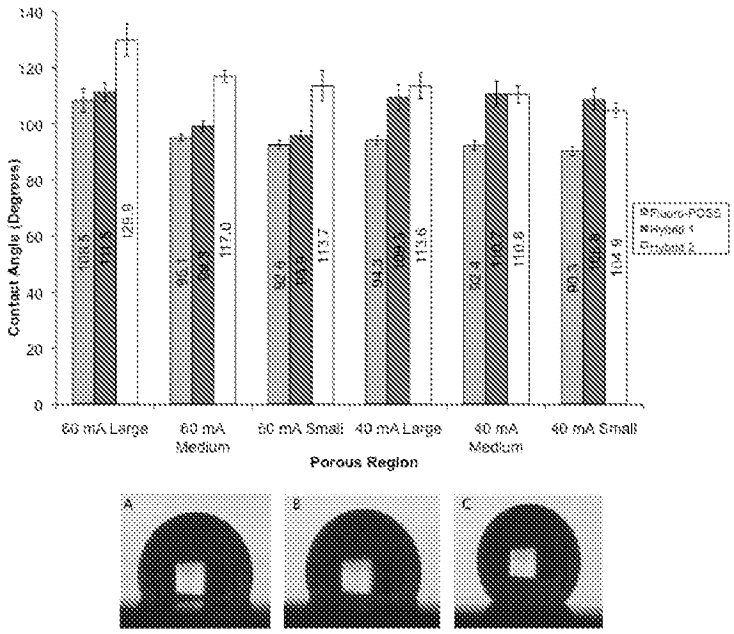

Figure 5: Comparison of contact angle of surface coatings on the 60 mA and 40 mA lateral etches and photographs of sessile water droplets on the 60 mA large pore region from (A) FluoroPOSS, (B) Hybrid 1 and (C) Hybrid 2. (error bars shown are +/- the standard deviation)

.

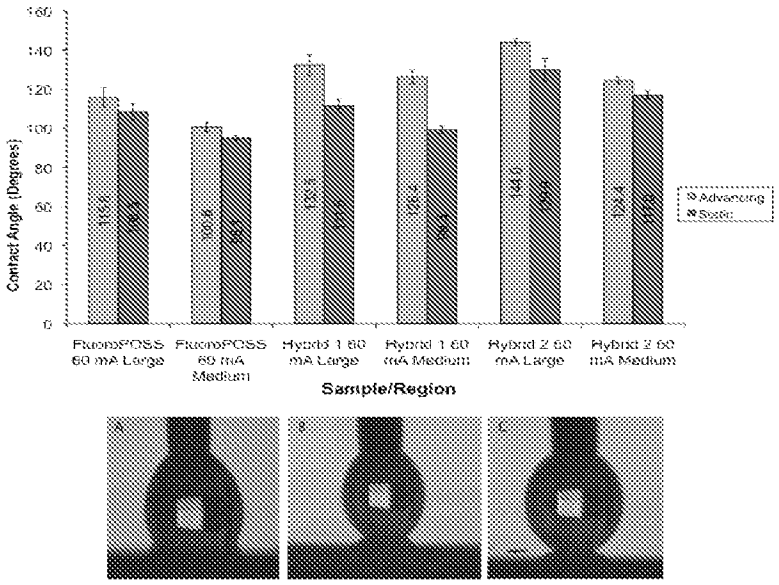

Figure 6: Advancing contact angles on the two largest pore regions for each surface functionalisation and photographs of sessile water droplets on the 60 mA large pore region for (A) FluoroPOSS, (B) Hybrid 1 and (C) Hybrid 2. (error bars shown are +/- the standard deviation)

Hybrid 2 with a maximum static contact angle of 130° outperforms Hybrid 1 (ca 111°) in terms of maximum contact angle achieved (Figure 5). This is most likely due to the orientation of the FluoroPOSS groups in each sample. As observed from our previous work based on thin films of these materials on flat silicon wafer

surfaces [19], the FluoroPOSS component tends to predominantly migrate to the thin film-air interface in Hybrid-2, whereas it remains mostly in the substrate-thin film interface on the Hybrid-1 surface. Hence, the higher contact angle observed with the Hybrid-2 sample is attributed to the migration of FluoroPOSS component onto the surface. Our previous work with fluorosilanes [18] has shown that static contact angle analysis on highly hydrophobic surfaces leads to contact angle value of <130°. This is due to the inability of the drop to dispense from the hydrophobic Teflon coated syringe. In order to place the drop on the surface and collect static contact angle data the droplet usually undergoes some form of deformation, either splatting if dropped or undergoing relaxational distortion if the needle is removed. For this reason, the regions that showed the highest contact angles were investigated by advancing contact angle analysis. This allows the drop to remain attached to the needle (Figure 6) and hence gives a more accurate idea of the contact angle created by the hydrophobic surfaces. Figure 6 shows the comparison of the static contact and advancing contact angles for the two largest pore regions with each surface functionalisation.

A definite increase was seen in contact angles for all surfaces measured by advancing analysis compared to static contact angle analysis. These advancing contact angle (CA) measurements are more reliable and better reflect the true hydrophobicity of the surfaces. The advancing CA analysis showed the same trend as static analysis with Hybrid 2 showing higher hydrophobicity than Hybrid 1 and the FluoroPOSS, and the advancing angles increased as the pore size increased. The contact angles measured for Hybrid 2 on the largest pore region (ca. 144°) are also comparable to our previous work with fluorosilane functionalisation (ca 147°). However, in both cases we were still unable to reach true superhydrophobicity (contact angle >150°).

4. CONCLUSIONS

We have created gradients with porous architectures ranging from the micro to nanoscale regimes via the use of asymmetric pSi preparation and functionalized these surfaces by dip-coating in various fluoro polymer solutions. Combining the optimal dip-coating conditions and surface chemistry with porosity gradients we were able to substantially increase the contact angle from 102° to 144° (Hybrid 2). As we are working with hydrophobic surface chemistries we saw that the increasing pore sizes increased the hydrophobicity of the surface, consistent with the Cassie-Baxter Model. The use of our gradient format has allowed the production of near superhydrophobic surfaces and is also a convenient format to be used for the screening of surface properties for applications in low-fouling and self-cleaning materials.

ACKNOWLEDGMENTS

The authors acknowledge the financial support of the Australian Research Council (ARC) to carry out the research.

REFERENCES

[1] B. E. Collins, K. P. S. Dancil, G. Abbi, and M. J. Sailor, "Determining Protein Size Using an Electrochemically Machined Pore Gradient in Silicon". Adv. Funct. Mater 12(3), 187-191 (2002).

[2] J. Genzer and K. Efimenko, "Recent developments in superhydrophobic surfaces and their relevance to marine fouling: a review". Biofouling 22(5), 339 - 360 (2006).

[3] X. Zhang, F. Shi, J. Niu, Y. Jiang, and Z. Wang, "Superhydrophobic surfaces: from structural control to functional application". J. Mater. Chem 18(6), 621-633 (2008).

[4] W. Barthlott and C. Neinhuis, "Purity of the sacred lotus, or escape from contamination in biological surfaces". Planta 202(1), 1-8 (1997).

[5] X. J. Feng and L. Jiang, "Design and Creation of Superwetting/Antiwetting Surfaces". Adv. Mater 18(23), 3063-3078 (2006).
[6] S. Jayaprakash, J. D. Samuel, and J. Ruhe, "A Facile Photochemical Surface Modification Technique for the Generation of Microstructured Fluorinated Surfaces" Langmuir. 20(23), 10080-10085 (2004).
[7] N. Zhao, Q. Xie, X. Kuang, S. Wang, Y. Li, X. Lu, S. Tan, J. Shen, X. Zhang, Y. Zhang, J. Xu, and C. C. Han, "A Novel Ultra-hydrophobic Surface: Statically Non-wetting but Dynamically Non-sliding". Adv. Funct. Mater 17(15), 2739-2745 (2007).
[8] S. Krishnan, R. Ayothi, A. Hexemer, J. A. Finlay, K. E. Sohn, R. Perry, C. K. Ober, E. J. Kramer, M. E. Callow, J. A. Callow, and D. A. Fischer, "Anti-Biofouling Properties of Comblike Block Copolymers with Amphiphilic Side Chains". Langmuir 22(11), 5075-5086 (2006).
[9] Y. Ofir, B. Samanta, P. Arumugam, and V. M. Rotello, "Controlled Fluorination of FePt Nanoparticles: Hydrophobic to Superhydrophobic Surfaces". Adv. Mater 19(22), 4075-4079 (2007).
[10] Joseph M. Mabry, A. Vij, Scott T. Iacono, and Brent D. Viers, "Fluorinated Polyhedral Oligomeric Silsesquioxanes (F-POSS)13". Angew. Chem. Int. Ed 47(22), 4137-4140 (2008).
[11] L. E. Moody, D. Marchant, W. W. Grabow, A. Y. Lee and J. M. Mabry, "Determination of Nanocomposite Mechanical and Surface Properties of Semicrystalline Polymer Blends with POSS", SAMPE 2005 Fall Technical Conference (2005).
[12] J. M. Mabry, D. Marchant, B. D. Viers, P. N. Ruth, S. Barker and C. E. Schlaefer In Fluoropolymer property enhancement via incorporation of fluorinated polyhedral oligomeric silsesquioxanes (FluoroPOSS), International SAMPE Symposium and Exhibition, 2004; Society for the Advancement of Material and Process Engineering: 2004; pp 1316-1328
[13] A. Tuteja, W. Choi, M. Ma, J. M. Mabry, S. A. Mazzella, G. C. Rutledge, G. H. McKinley, and R. E. Cohen, "Designing Superoleophobic Surfaces". Science 318(5856), 1618-1622 (2007).
[14] G. K. Aravindaraj, N. R. Choudhury, and N. K. Dutta, "Fluoropolyurethane hybrid for thin film applications". Polymer Preprints 48(1), 686-687 (2007).
[15] R. Blossey, "Self-cleaning surfaces - virtual realities". Nature Mater 2, 301 (2003).
[16] K. Hwang, S. Kim, Y. Park, H. Jeon, and J. Jeong, "Laterally graded porous silicon optical filter fabricated by diffusion-limited etch process". Applied Optics 47(10), 1628-1631 (2008).
[17] Y. L. Khung, G. Barritt, and N. H. Voelcker, "Using continuous porous silicon gradients to study the influence of surface topography on the behaviour of neuroblastoma cells". Exp. Cell Res 314(4), 789-800 (2008).
[18] Y. L. Khung, M. A. Cole, S. J. P. McInnes, and N. H. Voelcker, "Control over wettability via surface modification of porous gradients". Proc. of SPIE 6799, 6799091-12 (2007).
[19] G. K. Aravindaraj, N. R. Choudhury, and N. K. Dutta, "Fluoro-silsesquioxane-urethane hybrid for thin film applications". Under revision, ACS: Appl. Mater. Interf 2008.
[20] A. Nakajima, Hashimoto, K., Watanabe, T., "Recent Studies on Superhydrophobic Films". Monatshefte fur Chemie 132, 31-41 (2001).
[21] P. Laoharojanaphand, T. J. Lin, and J. O. Stoffer, "Glow Discharge Polymerization of Reactive Functional Silanes on Poly (methyl Methacrylate)". J. Appl. Polym. Sci 40, 369-384 (1990).
[22] D. T. Clark and A. Dilks, "ESCA Applied to Polymers. XXIII. RF Glow Discharge Modification of Polymers in Pure Oxygen and Helium-Oxygen Mixtures". J. Polym. Sci. Pol. Chem 17, 957-976 (1979).
[23] A. G. Kannan, N. R. Choudhury, and N. K. Dutta, "Synthesis and characterization of methacrylate phospho-silicate hybrid for thin film applications". Polymer 48(24), 7078-7086 (2007).
[24] J. Li, Fu, Y., Cong, Y., Wu, L., Han, Y., "Macroporous fluoropolymeric films templated by silica colloidal assembly. A possible route to superhydrophobic surfaces". Applied Surface Science 252, 2229-2234 (2006).
[25] F. Cebeci, Wu, Z., Zhai, l., Cohen, R., Rubner, M., "Nanoporosity-driven superhydrophilicity: A means to create multifunctional antifogging coatings". Langmuir 22, 2856-2862 (2006).
[26] G. McHale, Shirtcliffe, N., Aqil, S., Perry, C., Newton, M., "Topography driven spreading". Physical review Letters 93 (2004).
[27] N. Shirtcliffe, McHale, G., Newton, M., Perry, C., Roach, P., "Porous materials show superhydrophobic to superhydrophilic switching". Chemical Communications 3135-3137 (2005).
[28] R. Narhe, Beysens, D., "Water condensation on a super-hydrophobic spike surface". Europhysics Letters 75, 98-104 (2006).